

NASA Technical Memorandum 88940

Thermomechanical Behavior of Plasma-Sprayed ZrO_2 - Y_2O_3 Coatings Influenced by Plasticity, Creep, and Oxidation

J. Padovan and B.T.F. Chung
University of Akron
Akron, Ohio

and

Glen E. McDonald, and Robert C. Hendricks
Lewis Research Center
Cleveland, Ohio

Prepared for the
11th Annual Conference on Composites, Advanced Ceramics,
and Composite Materials
cosponsored by the American Ceramic Society, DOD, and NASA
Cocoa Beach, Florida, January 18-23, 1987



Thermomechanical Behavior of Plasma-Sprayed ZrO_2 - Y_2O_3 Coatings
Influenced by Plasticity, Creep, and Oxidation

J. Padovan and B.T.F. Chung
University of Akron
Akron, OH 44325

and

Glen E. McDonald and Robert C. Hendricks
National Aeronautics and Space Administration
Lewis Research Center
Cleveland, Ohio 44135

ABSTRACT

Thermocycling of ceramic-coated turbomachine components produces high thermomechanical stresses that are mitigated by plasticity and creep but aggravated by oxidation, with residual stresses exacerbated by all three. These residual stresses, coupled with the thermocyclic loading, lead to high compressive stresses that cause the coating to spall. In this paper a ceramic-coated gas path seal is modeled with consideration given to creep, plasticity, and oxidation. The resulting stresses and possible failure modes are discussed.

INTRODUCTION

Thermal and corrosion-protective coatings applied to the hot-section components of gas turbines can improve engine efficiency and extend component life. Much of the extensive research to ascertain the thermomechanical behavior of thin coatings applied to vanes, blades, and rocket engines and thick coatings applied to seals and static components has been summarized in reference 1. Simplified models have shown that large thermal stresses are induced during initial startup. Once startup is complete, long-term effects can dominate. These include plastic flow (creep), debonding (delamination), crack growth initiation, and oxidation (where debonding and crack growth also occur in the startup phase). These issues are formulated and discussed in detail in reference 2. Herein the thermomechanical effects (discussed in ref. 1) are summarized, and the calculated stresses due to oxide formation for long-term thermal soaking are discussed.

RESULTS AND DISCUSSION

Through the use of a constrained Newton-Raphson type of time-marching scheme, the thermoelastic/plastic/creep behavior of a graded-ceramic-coated gas turbine seal was analyzed (fig. 1). The generality of the scheme developed is such that inelastic strains in ceramics due to creep and plasticity can be determined in both single- and multiple-cycle environments. This includes the capability of handling thermal ratcheting and the concomitant residual stress/strain fields. From the results of numerical examples for a thermal cycle consisting of a 1.2-sec ramp from ambient to power, 10 min at power, and a

1.2-sec ramp to ambient, the calculated stresses given in figures 2 to 4 can be summarized as follows:

(1) Severe stresses are generated in the interface zone between the metal substrate and the first ceramic layer.

(2) Plasticity behavior appears to predominate creep effects in the ceramic laminae closest to the substrate.

(3) Plastic and creep effects tend to combine to reduce surface stress in the exposed (hot gas) ceramic layer.

(4) The largest residual stresses occur in the interface region.

The oxidation/scaling of metal surfaces typically involves complex diffusion and chemical interactions. Protective coatings often have imperfections that permit oxygen diffusion and subject the system to corrosive attack. Here we assume the attack to occur in the bond region between the ceramic and the substrate. Similar to creep, the overall oxidation process can be modeled by a power-law expression (ref. 3),

$$\frac{dx}{dt} = \kappa(T) f(x) \quad (1)$$

where the oxide is assumed to grow principally in a direction normal to the surface. The process involves the gradual etching of the metallic bond coat and the growth of metallic oxides of significantly different volume and thermo-mechanical properties (fig. 5). Given the thermal history of the bond coat $T_I(t)$, the overall thickness of the oxide x_{ox} , the amount of bond coat etched β , and the net interference χ , fit can be assessed (ref. 2.). Further, if $T_I(t)$ is constant, the simplified forms become

$$x_{ox} = \sqrt{2\kappa(T_I)t} \quad (2)$$

$$\beta = \alpha(T_I)x_{ox} \quad (3)$$

$$\chi = [1 - \alpha(T_I)]x_{ox} = x_{ox} - \beta \quad (4)$$

where α is an empirical thermal parameter relating rate of etching to rate of thickness change. In this model the rate drops off because the diffusion path for the oxygen has been enlarged by accumulation of oxide normal to the surface. To start the numerical calculations, an initial arbitrarily thin layer of oxide (0.025 mm; 0.001 in.) is assumed to exist. The governing field equations and their associated boundary conditions are derived in detail in reference 2.

The method was applied to ascertain the stress states representative of a ceramic-coated gas path seal (fig. 1) with the ceramic configuration of figure 6. Since the transient time from ambient to power was short and oxidation growth information was available for "oven soak" conditions, we ignored the transient phase and considered only a steady thermal loading. Here the internal temperature adjacent to the ceramic was 1315 °C (2400 °F), and the outside of the substrate held at 590 °C (1100 °F). With the solution flow

chart given in figure 7 various aspects of the thermomechanical oxidation problem are illustrated in figures 8 to 16.

Figure 8 depicts the overall growth of the oxide scale (herein assumed to be entirely Al_2O_3). As can be seen, the initial phase of oxidation is marked by rapid growth; but as the scale grows, the oxygen diffusion path is increased and scale growth diminishes. Figures 9 to 11 illustrate the stresses in various layers. In the metallic substrate layer tensile stresses increase as the scale grows (fig. 9). Similar effects occur in the bond coat (fig. 10). In the ceramic layer the stresses are progressively driven into the compressive zone (fig. 11). High tensile stress also occurs in the scaling layer, where it builds up with "thermal soak" time (fig. 12). This is especially true in the early stages of oxidation. Very high tensile stresses are noted even for small levels of scaling. Perhaps these stress can be more readily understood by thinking of an interference fit between the ceramic inner cylinder and the oxide/bond coat/substrate outer cylinder. As the oxide grows, it is assumed to become a part of the outer cylinder, which expands because of oxide growth normal to the surface. Thus compressive stresses develop in the inner cylinder (ceramic) and force tensile stresses in the outer cylinder.

The buildup of residual stress fields is important to coating longevity. Knowing the oxide growth and considering an isothermal system we could estimate the residual stresses (i.e., the imposed thermal gradient was set to zero and the stresses were calculated). The residual stresses may be thought of in another way. If two specimens of a material, one with oxide and the other without, could be completely stress relieved and a thermal load imposed, the difference in stresses at time zero would represent the residual stress. The magnitude of these stresses is illustrated in figures 13 to 16. As can be seen, fairly significant stresses can be generated, particularly in the ceramic and the scale. These stresses in combination with the steady and transient fields can shorten coating system life. In this analysis we have assumed oxide growth normal to the surface and elastic materials behavior. In the future we will investigate the effects of material inelasticity combined with the effects of oxidation. Such effects are of particular importance for long-term exposures to high-temperature environments.

SUMMARY

The extreme elastic stresses generated in thermocycling the hot-section components of gas turbines are mitigated by plasticity and creep effects. However, the residual stresses are increased. A model of the oxide layer growth was applied to a ceramic-coated gas path seal geometry. The model illustrates intense stress buildup even for very thin oxides and residual stress buildup at each interface with time. It remains to be demonstrated if inclusion of inelastic behavior will mitigate these oxide stresses and further if bond-coat imperfections are the key to localized oxidation and subsequent spallation.

REFERENCES

1. Mullen, R.L., Padovan, J., Braun, M.J., Chung, B.T.F., McDonald, G., and Hendricks, R.C., "Thermomechanical Design Criteria for Ceramic-Coated Surfaces," (6th CIMTEC World Congress on High Technology Ceramics, Milan, Italy, 23-28 June 1986.) NASA TM-87328, 1986.

2. Padovan, J., Chung, B.T.F., and Braun, M.J., "Analysis of Thermo-Mechanical Response of Thick Thermal Protective Coating Systems," University of Akron, Akron, OH, NASA Grant NAG3-265, Aug. 1986.
3. Hauffe, K., Oxidation of Metals. Plenum Press, New York, 1965.

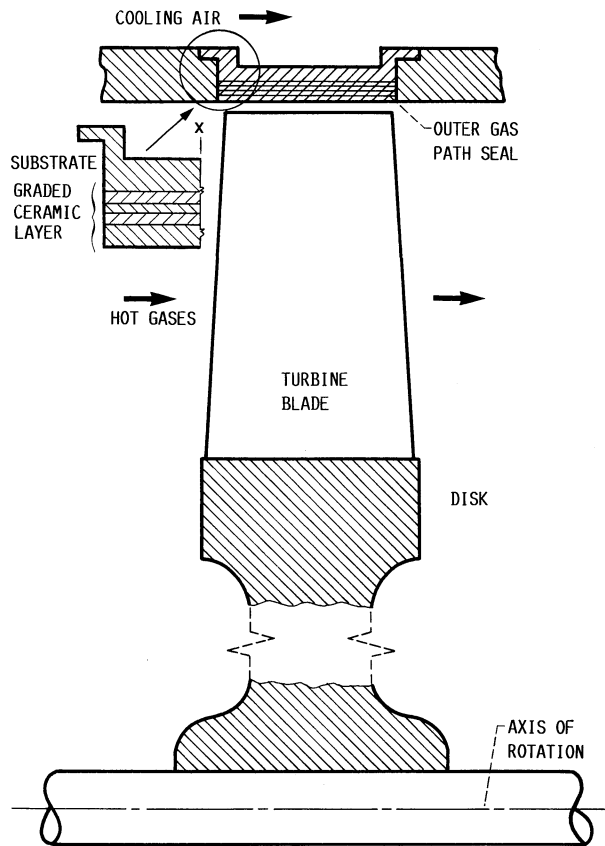


FIGURE 1.- CROSS SECTION OF GAS TURBINE.

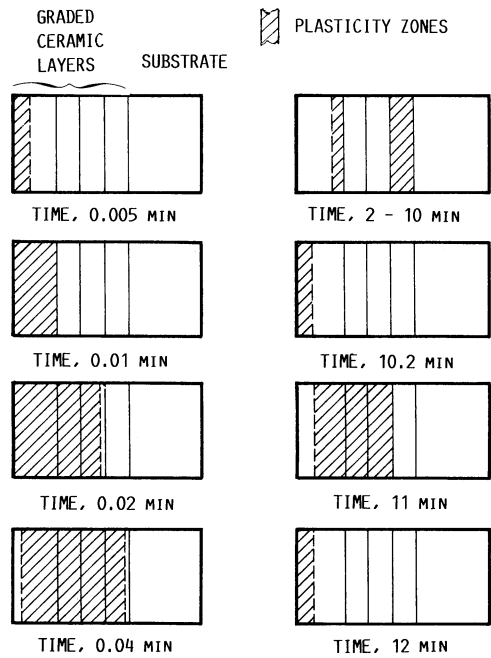


FIGURE 2.- GROWTH AND SUBSIDENCE OF PLASTICIZED ZONES DURING THERMAL CYCLE.

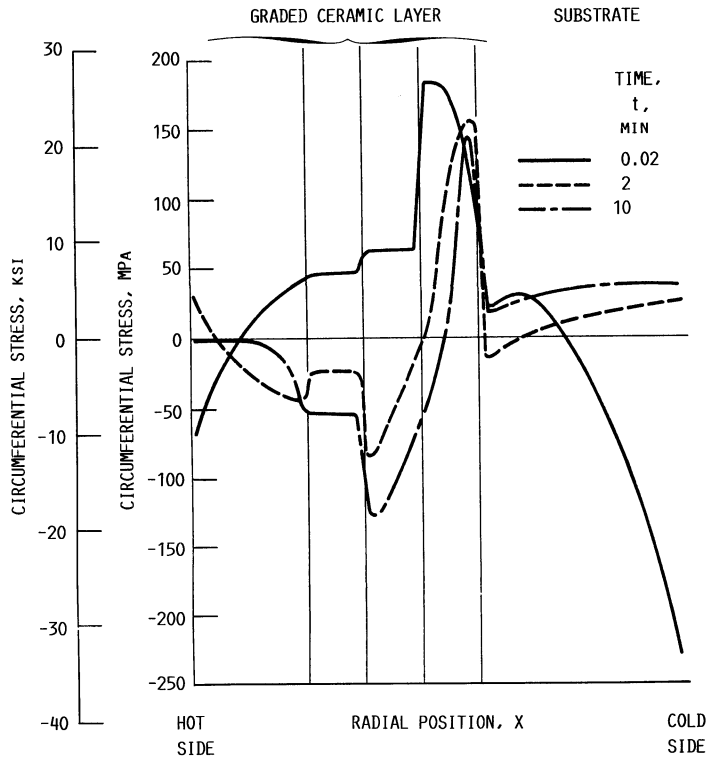


FIGURE 3. - STRESS STATE OF CROSS-SECTIONAL FIELD DURING HEATUP.

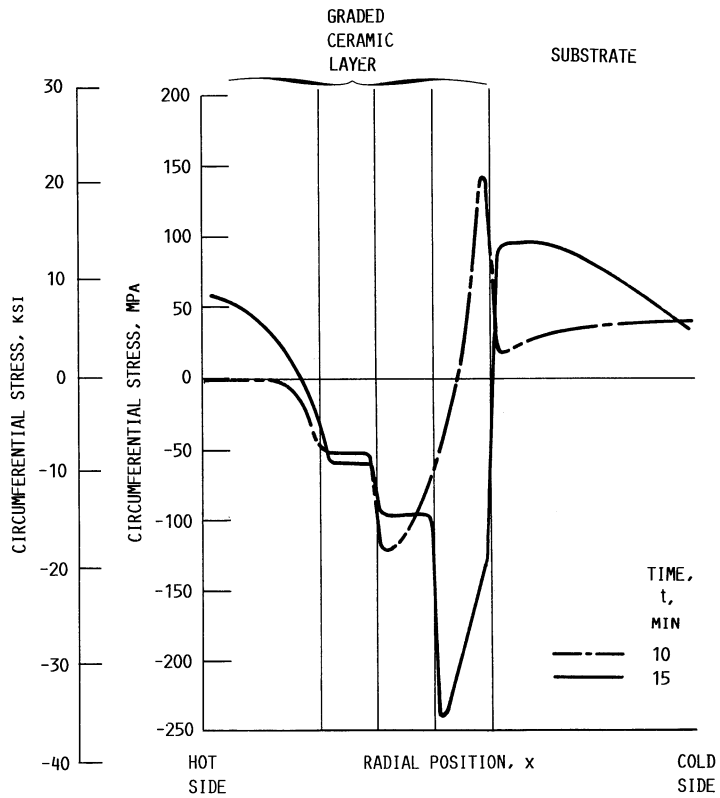


FIGURE 4. - STRESS STATE OF CROSS-SECTIONAL FIELD DURING COOLDOWN.

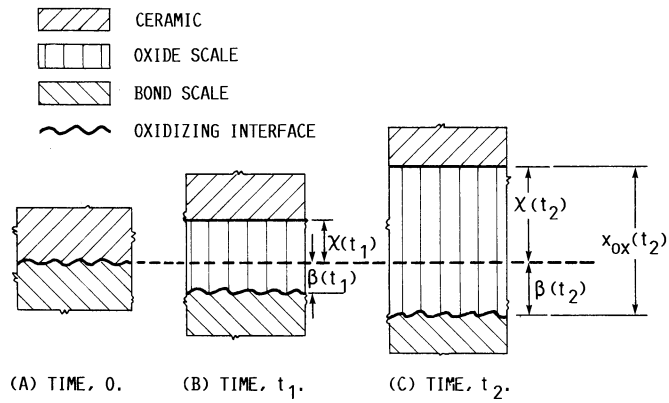


FIGURE 5.- GROWTH OF OXIDE SCALE AT BOND COAT/CERAMIC INTERFACES ($0 < t_1 < t_2$).

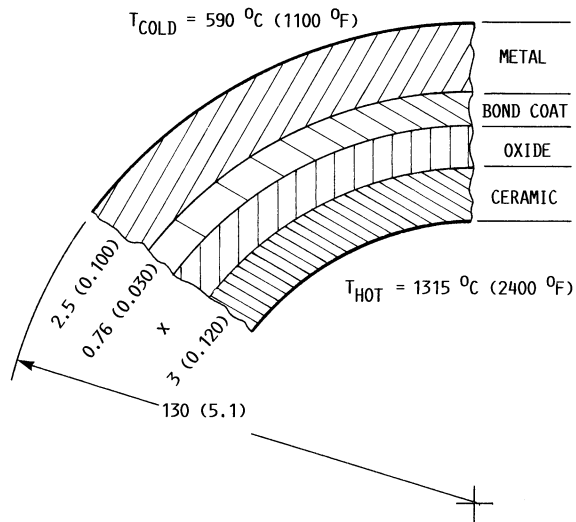


FIGURE 6. - LAMINATE GEOMETRY OF OUTER GAS PATH SEAL. (DIMENSIONS ARE IN MILLIMETERS (INCHES).)

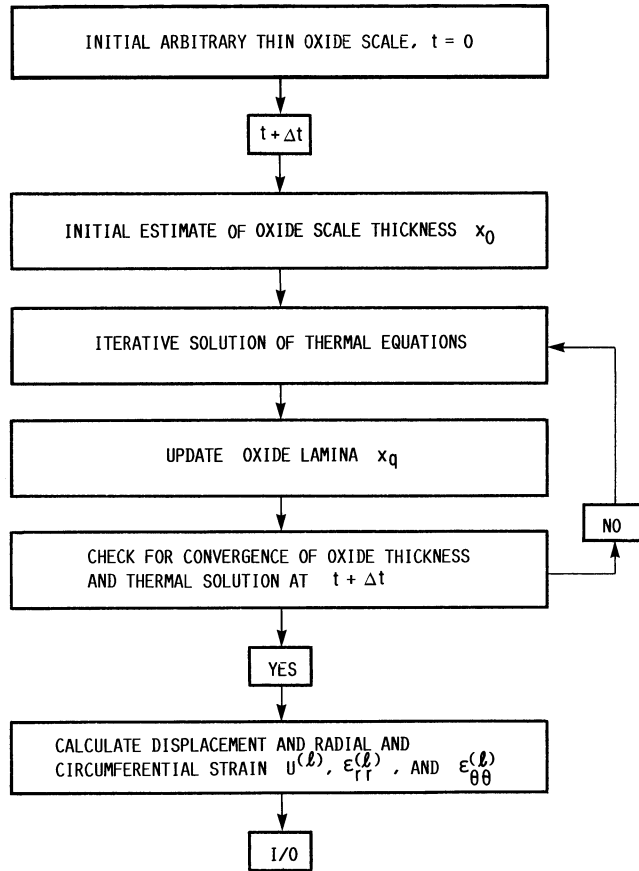


FIGURE 7.- FLOW CHART OF SOLUTION SCHEME.

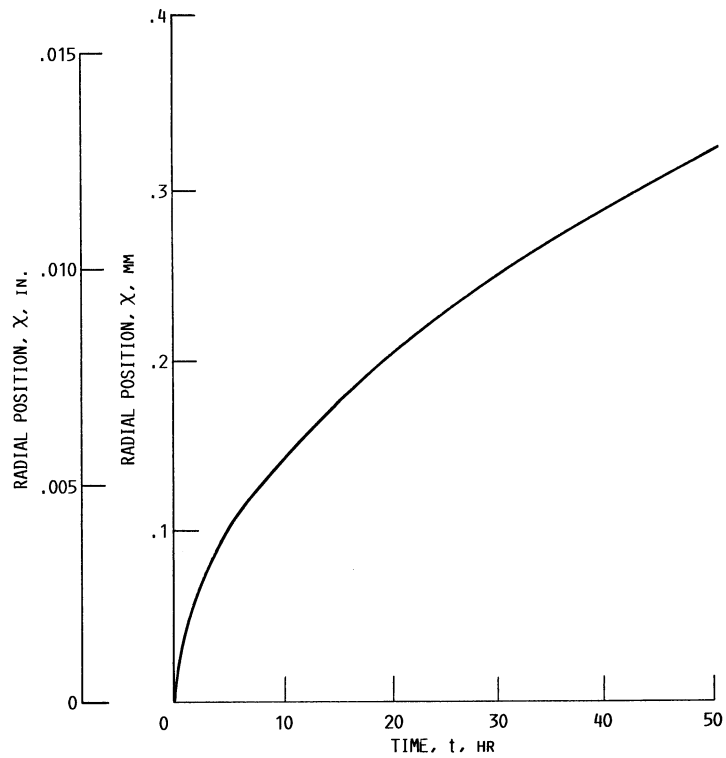


FIGURE 8.- SCALE GROWTH WITH TIME.

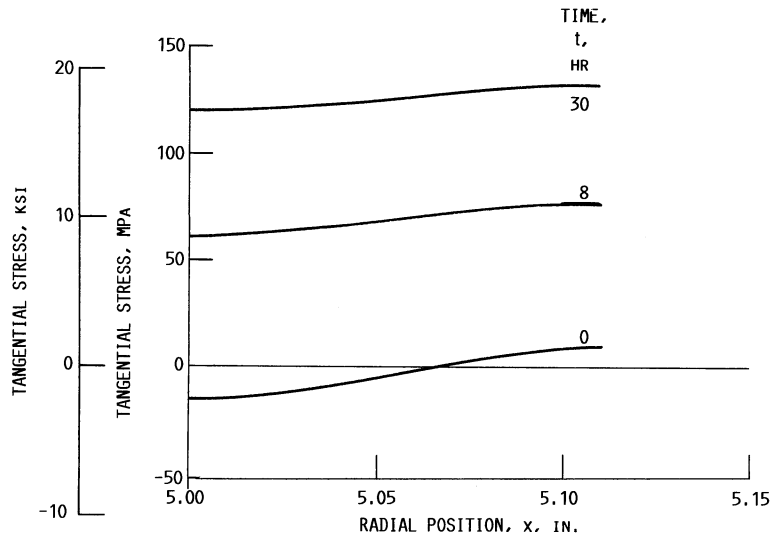


FIGURE 9.- STRESS STATE IN METAL SUBSTRATE.

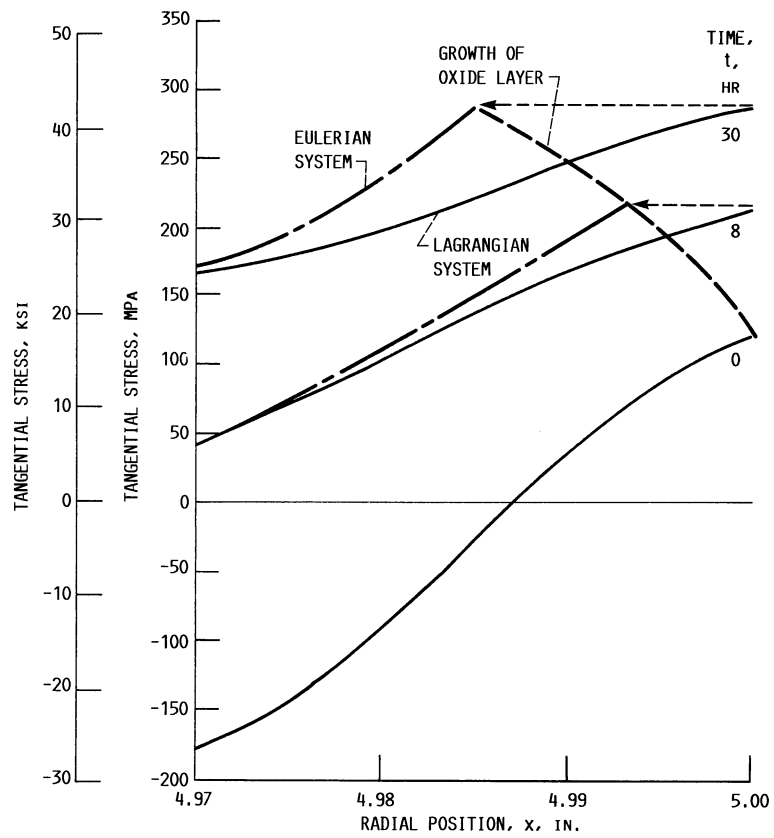


FIGURE 10.- STRESS STATE IN BOND COAT.

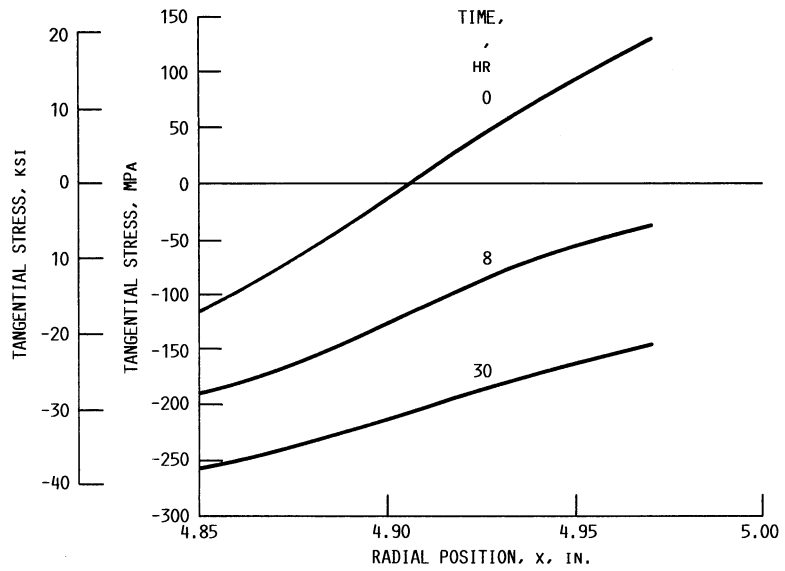


FIGURE 11. - STRESS STATE IN CERAMIC COATING.

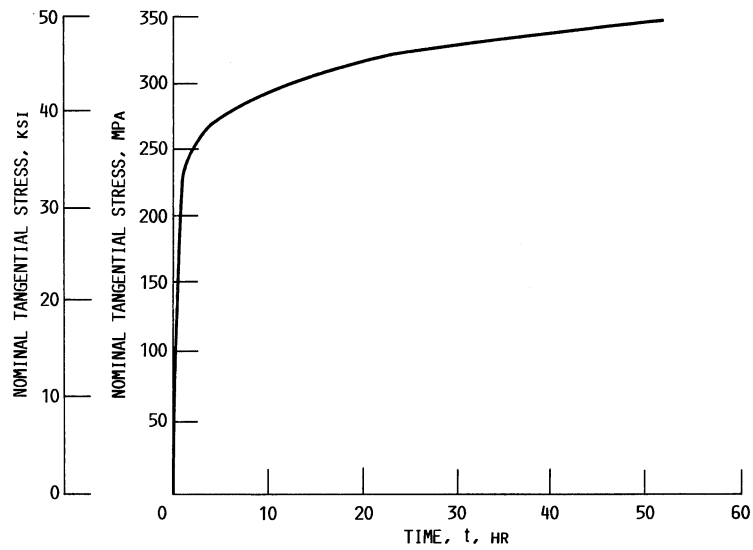


FIGURE 12.- NOMINAL STRESS STATE IN OXIDE SCALE.

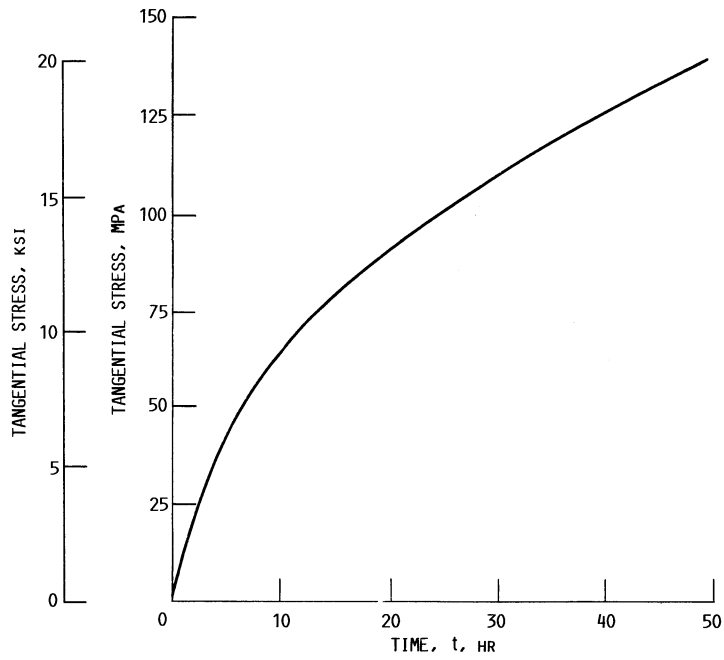


FIGURE 13.- MAXIMUM RESIDUAL STRESS IN METAL SUBSTRATE.

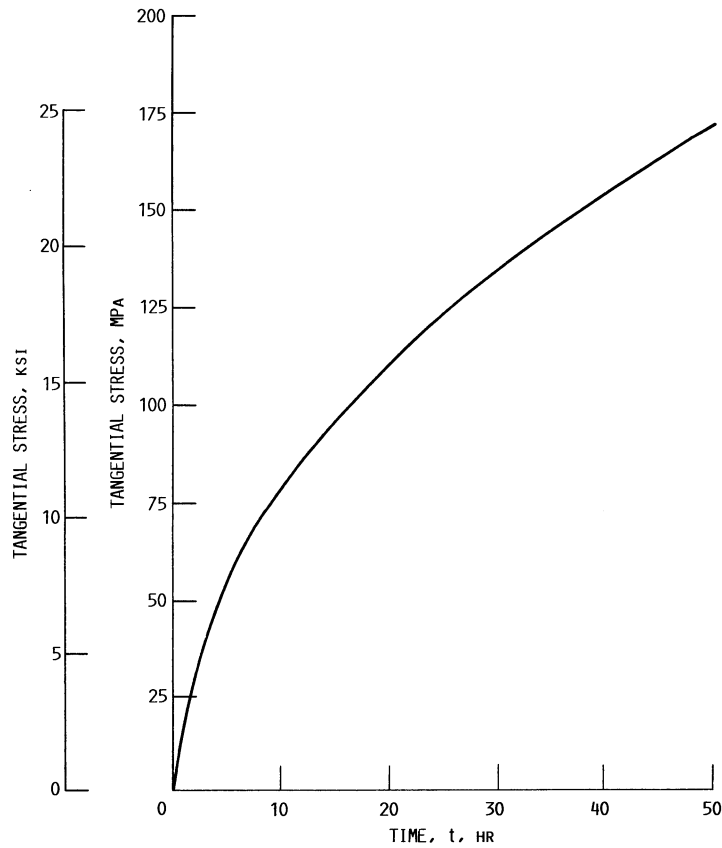


FIGURE 14.- MAXIMUM RESIDUAL STRESS IN BOND COAT.

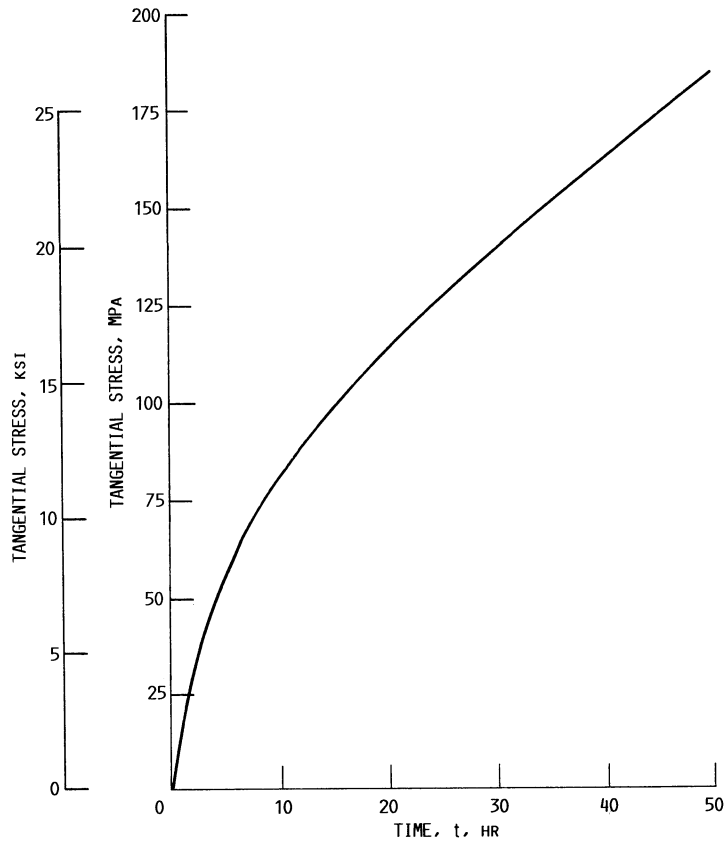


FIGURE 15.- MAXIMUM RESIDUAL STRESS IN CERAMIC COATING.

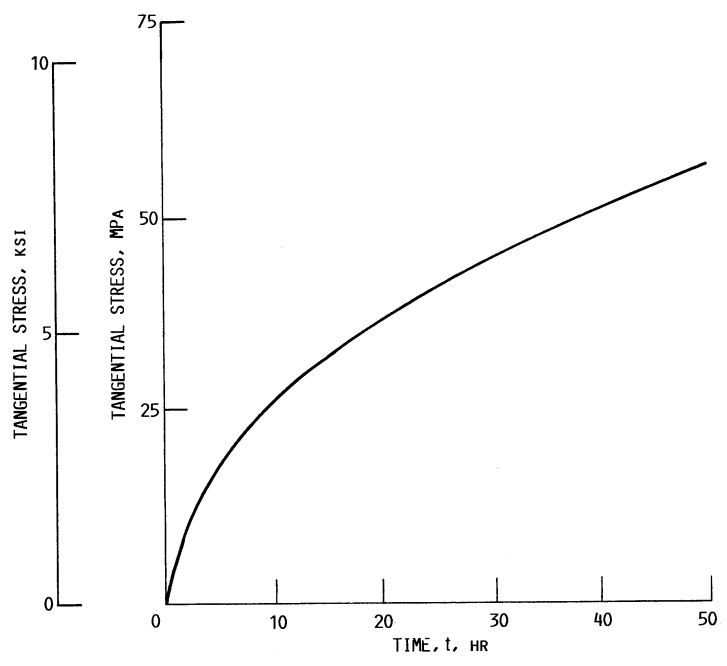


FIGURE 16.- MAXIMUM RESIDUAL STRESS IN OXIDE SCALE.

1. Report No. NASA TM-88940	2. Government Accession No.	3. Recipient's Catalog No.	
4. Title and Subtitle Thermomechanical Behavior of Plasma-Sprayed ZrO₂-Y₂O₃ Coatings Influenced by Plasticity, Creep, and Oxidation		5. Report Date January 1987	
		6. Performing Organization Code 553-13-00	
7. Author(s) J. Padovan, B.T.F. Chung, Glen E. McDonald, and Robert C. Hendricks		8. Performing Organization Report No. E-3385	
		10. Work Unit No.	
9. Performing Organization Name and Address National Aeronautics and Space Administration Lewis Research Center Cleveland, Ohio 44135		11. Contract or Grant No.	
		13. Type of Report and Period Covered Technical Memorandum	
12. Sponsoring Agency Name and Address National Aeronautics and Space Administration Washington, D.C. 20546		14. Sponsoring Agency Code	
		15. Supplementary Notes Prepared for the 11th Annual Conference on Composites, Advanced Ceramics, and Composite Materials, cosponsored by the American Ceramic Society, DOD, and NASA, Cocoa Beach, Florida, January 18-23, 1987. J. Padovan and B.T.F. Chung, Univer- sity of Akron, Dept. of Mechanical Engineering, Akron, Ohio 44325; Glen E. McDonald and Robert C. Hendricks, NASA Lewis Research Center.	
16. Abstract Thermocycling of ceramic-coated turbomachine components produces high thermo- mechanical stresses that are mitigated by plasticity and creep but aggravated by oxidation, with residual stresses exacerbated by all three. These residual stresses, coupled with the thermocyclic loading, lead to high compressive stresses that cause the coating to spall. In this paper a ceramic-coated gas path seal is modeled with consideration given to creep, plasticity, and oxida- tion. The resulting stresses and possible failure modes are discussed.			
17. Key Words (Suggested by Author(s)) Ceramics; Oxidation; Creep; Plasticity; Coatings		18. Distribution Statement Unclassified - unlimited STAR Category 34	
19. Security Classif. (of this report) Unclassified	20. Security Classif. (of this page) Unclassified	21. No. of pages 13	22. Price* A02